

FINE DETAILS ON THE SELECTIVITY AND KINETICS OF THE FISCHER-TROPSCH SYNTHESIS OVER PRECIPITATED COBALT CATALYSTS BY COMBINATION OF QUANTITATIVE GAS CHROMATOGRAPHY AND MODELLING.

Ronald S. Hurlbut, Imre Puskas and Daniel J. Schumacher
Amoco Corporation, Naperville, Illinois 60566, (708) 653-4897

Keywords: Fischer-Tropsch, chain growth, kinetics, diffusion.

INTRODUCTION.

This report summarizes a part of our work carried out on the conversion of natural gas-derived synthesis gas to liquid fuels. Particularly, we were interested to find a catalyst which can convert dilute synthesis gas -such as obtainable from natural gas by partial oxidation with air- to predominantly liquid products at low pressures. For this purpose we needed to generate fundamental kinetic information on the controllability of the molecular weight distribution, which is defined by the chain growth probability of the reaction, because relatively little information is available on the subject (1-5). A wealth of information suggests, that with some exceptions in the low molecular weight regimes (1,6), the product distributions can be described by Anderson-Schulz-Flory (ASF) kinetics, using either a single chain growth probability, or separate chain growth probabilities for the light and heavy products (7). The causes of the "dual" chain-growth probabilities still have not been defined. Three causes have been suggested which could account for the dual chain growth probabilities: 1./ Differences in the catalytic sites (8,9); 2./ transport-enhanced 1-olefin readsorption and incorporation into the heavy product fractions (10); 3./ operating characteristics of the reactor (3).

To aid with our objectives, we have developed an approach for product analyses which is based on a combination of quantitative gas chromatography and modelling. This resulted in instantaneous determinations of the complex product mixtures, providing an opportunity to generate instantaneous information on the selectivity and the kinetics of the reaction. The influence of experimental parameters (feed, pressure, space velocity and temperature) on the chain growth probability and on the rate was studied by this analytical approach. The results shed new information on the causes of the deviations from the ASF kinetics. Furthermore, the kinetic data also provide evidence for diffusional limitations of the reaction rates. Finally, the instantaneous analyses may aid in future research to link the kinetics and the selectivity of the reaction which seem to be interdependent and hence should require simultaneous treatment.

EXPERIMENTAL SECTION.

The methods of catalyst preparation, characterizations, evaluations and product analyses have been outlined in previous publications (6, 11-13). Full details are given in the unabbreviated version of this paper.

RESULTS AND DISCUSSIONS.

1./ Feed composition studies.

The addition of extra hydrogen to the feed was evaluated on Catalyst 1 in an experiment conducted at 197°C, 156 kPa. Table 1 gives the detailed results. Table 1 also serves to illustrate the type of information generated by the GC-modelling combination. The data show that an increase of the H₂ to CO feed ratio from 2.0 to 3.1 resulted in substantial increase of the reaction rate as indicated by the catalyst productivities, and a modest decrease in the growth factor. The data also illustrate how the C₁ to C₄ product selectivities, expressed in percentage of the theoretical ASF predictions, change with the H₂ to CO feed ratio. The C₁ selectivity is very dependent on the feed ratio. However, the C₂ to C₄ selectivities are only little influenced by the feed ratio. This is in line with our earlier findings (6), that over Co catalysts, the fraction of C₂ to C₄ olefin incorporation by telomerization is nearly constant and little influenced by the experimental variables. The data of Table 1 suggest, that high H₂ to CO feed ratio promotes the hydrogenation of the C₂-C₄ olefins slightly more than their telomerization.

We considered the possibility that physisorbing inert components of the feed may also impact on the value of the growth factor by

creating "steric impediment" to propagation on the surface of the catalyst. This possibility was studied by nitrogen dilution of the feed on Catalyst 2, at 202°C, 168 kPa. The highlights of the results are shown in Figure 1. Indeed, nitrogen dilution of the feed resulted in decreased growth and decreased rate (productivity). Since nitrogen dilution also resulted in increased space velocity, specifically from 131 to 177 VHSV, the possibility need to be considered that the observed changes may have been caused by space velocity changes rather than by nitrogen dilution. It will be demonstrated later, that increased feed space velocity results in increased rate, without affecting the growth factor. Hence we can conclude that nitrogen dilution was the cause of the lower reaction rate and lower growth factor.

If nitrogen dilution affects the chain growth, it is expected, that the hydrocarbon products of the synthesis may also have a similar effect. The effect of hydrocarbon dilution was studied by comparing the reaction products from one-pass operations and from recycle mode operations. In this latter mode, the reaction products were passed through an air-cooled condenser to condense out the liquids. Part of the uncondensed gases were pumped back into the reactor after mixing with fresh feed. Catalyst 3 was used in the experiments, at 200.5°C, 103 kPa, with identical fresh feed flows. In the once-through operations, we obtained 60.4% CO conversion, 11.8% methane selectivity, 0.732 growth factor and 0.0235 g/g/hr catalyst productivities. During recycle operations, with 1.9 to 1 volumetric recycle to fresh feed ratio, we obtained 58.2% CO conversion, 13.2% methane selectivity and 0.0223 g/g/hr catalyst productivity. Unfortunately, the gas chromatographic effluent analysis was not adoptable for the determination of the growth factor on the basis of the C₁ to C₁₀ products, because these were partially removed by the recycle operations. We estimate 0.725 growth factor for the recycle operations on the basis that it yields the same selectivity balance as obtained in the once-through operations. We believe that these results qualitatively demonstrate that hydrocarbon dilution of the feed results in decreased growth and decreased rate, because the inert diluents successfully compete with the chemisorbing reagents for the catalytic sites.

2./ Pressure effects.

Table 2 illustrates the effect of small pressure changes at constant temperatures and constant feed flow rates on three different catalysts. In all cases, significant increases in the growth factor and also in the rates (catalyst productivities) were caused by small pressure increases. The C₁ to C₄ carbon selectivities (not shown in the Table) followed the trends defined by the growth factors. However, the C₁ to C₄ selectivities expressed in percent of their theoretical values did not appear to change. The small scatter of data is attributable to analytical error; no trend can be recognized with the pressure changes.

3./ Space velocity effects.

The effect of space velocity changes was studied on Catalyst 6 in atmospheric experiments at 195°C. The results are summarized in Figures 2 to 8. As Figure 2 shows, in this series of experiments we obtained essentially 100% selectivity balances, indicating that the ASF model extrapolation adequately accounted for the heavy products. Figure 2 also shows that the space velocity had little, if any effect on the growth factor. The data of Figure 3 illustrate another interesting point. While the CO conversion increased with increasing contact time (i.e. decreasing space velocity), the catalyst productivity decreased. Since the reaction occurs on the catalyst surface, and the feed composition, temperature and pressure were identical in this series of experiments, the change in catalyst productivity (rate) must have been caused by changes in the diffusion rates of the reagents to reach the catalyst surface. Faster space velocity provided faster diffusion rates. From these results, diffusional limitations of the reaction rates can be inferred.

Figures 4 to 8 show the C₁ to C₄ product selectivity dependencies on the contact time. These appear to be independent of the contact time. However, as expected, the distribution of the C₃ and C₄ products changes. The propylene and 1-butene contents decrease with increasing contact time due to hydrogenations to

propane and butane, respectively, and, in case of 1-butene, also to isomerizations to cis- and trans-2 butenes (Figures 6 to 8).

4./ Temperature effects.

The effect of temperature changes was studied at constant pressure (156 kPa) and constant space velocity (120 VHSV) on Catalyst 1. As Figure 9 illustrates, in the 190-205°C region, the growth factor steeply increased with decreasing temperature. However, below about 180°C, the measured growth factors did not seem to change with decreasing temperature. The carbon selectivity balances, also shown in Figure 9, may shed some information about the causes of these observations. Above about 190°C, the carbon balances were in the 91-95 percent range, suggesting that extrapolation by the ASF model underestimated the heavy product formation. Below about 185°C, the heavy product formation was substantially underestimated as revealed by the balance data. Hence we infer, that at decreasing temperature, heavier products with very high value of growth factor may have continued to form, but these had little impact on the relative amounts of C₁ to C₁₀ products which provided the basis for the determination of the growth factor. The data seem to support the theories, that the measured growth factor is a composite of a wide range of actual growth factors.

Figures 10 to 12 illustrate, that the methane selectivities, expressed in percent of the theoretical, increase with increasing temperature, but the C₂, C₃ and C₄ selectivities are unaffected. However, temperature affects the C₂ and C₄ distributions. At higher temperatures less propene (Figure 11) and less 1-butene (Figure 12) were found.

Figure 13 shows the temperature dependance of the CO conversions and the catalyst productivities. Surprisingly, the results suggest a linear correlation between temperature (T) and rate (-r), except for the high temperature (high conversion) regions:

$$-r = k K (T - T_i) \quad (1)$$

where k is the rate constant, K is another constant characteristic for the conditions and T_i is the temperature of the start of the reaction. This means that the Arrhenius equation is not valid in this surface reaction. Nevertheless, in Figure 14, we present a pro-forma Arrhenius plot which is curved. (For the plot, we used CO conversion data in lieu of rate constants from the linear region of Figure 13). The results may not be surprising, because theoretical considerations have demonstrated that non-linear Arrhenius plots can be obtained in transport-limited catalytic reactions (14, 15). From the data, we estimate pro forma activation energies ranging from 16 to 31 kcal/mole, which cover the bulk of the previously reported values.

CHAIN GROWTH PROBABILITY AND PRODUCT SELECTIVITY.

We propose that the chain growth probability (α) is defined by the nature of the catalyst surface (C), the surface concentrations of the adsorbed species (S₁ to S_n) -which include chemisorbing reagents and non-reactive adsorbed species- and the temperature of the surface:

$$\alpha = f (C, S_1, \dots, S_n, T) \quad (2)$$

It may be expected, that the nature of the catalytic metal, the size of the metal crystallites, metal-support interactions may influence the chain growth probability. Indeed, different catalytic sites were postulated in the past to give different chain growth (8,9). However, providing evidence for this was elusive, but scientific interest continues in the subject. Our results demonstrated, that not only the chemisorbing reagents, but also the physisorbing inerts can affect the chain growth probability. The surface concentrations of the adsorbed species will depend on their respective concentrations in the gas phase, on the pressure, on their rate of chemisorption, and on the diffusional conditions.

Even though it may be a long way to define an explicit form for Equation 2, the Equation may be useful for some qualitative predictions. Even if a specific catalyst were to possess only one type of catalytic site, a common plug-flow type reactor will produce a multiplicity of growth factors due to changes in the relative surface concentrations of the adsorbing species along the reactor axis arising from gas-phase compositional changes.

and due to minor temperature gradients on the surfaces. We have modelled these possibilities and some results with relevant assumptions are shown. Figure 15 gives the calculated ASF plot of a product mixture with growth factor evenly changing from 0.70 to 0.80. For all practical purpose, the product mixture can be described by a single growth factor. However, a careful examination reveals a slight break in the ASF plot at C_9 - C_{10} . Figure 16 gives the ASF plots of two assumed mixtures. In one of the mixtures, the growth factor continuously changes from 0.60 to 0.85, in the other one from 0.60 to 0.95. In both examples, there is a break in the ASF plot around C_{10} . However, the C_6 to C_{10} data from the two plots are nearly parallel, yielding nearly identical growth factor values by the conventional measurements. With this example, we have simulated an explanation for the finding that the measured growth factor did not increase with decreasing temperature below about 185°C.

The above discussion makes it clear that the operating characteristics of the reactor can result in molecular weight distributions with non-linear ASF plots. However, our results do not provide any indication that "transport enhanced olefin readsorption" can lead to increased growth probability and to non-linear ASF plots, as postulated recently (10). In our work, we have found evidence only for C_2 - C_4 olefin incorporation, and possibly very little C_5 incorporation, but the degree of these incorporations was fairly constant and independent of the residence time.

REFERENCES.

1. Henrici-Olive, G., and Olive, S., *Angew. Chem. Intl. Ed. Engl.* 15, 136 (1976).
2. Dry, M. E., in "Catalysis Science and Technology" (J. R. Anderson and M. Boudart, Eds.), Springer Verlag, Berlin, 1981, p. 159. See also Idem, *Catal. Today*, 6, 183 (1990).
3. Matsumoto, D. K., and Satterfield, C. N., *Energy & Fuels* 3, 249 (1989).
4. Dictor, R. A., and Bell, A. T., *J. Catal.* 97, 121 (1986).
5. Krishna, K. R., and Bell, A. T., *J. Catal.* 139, 104 (1993).
6. Puskas, I., Hurlbut, R. S., and Pauls, R. E., *J. Catal.* 139, 139 (1993).
7. For a review, see Davis, B. H., *Preprints, ACS, Fuel Division*, 37, 172 (1992).
8. Huff, G. A., and Satterfield, C. N., *J. Catal.* 85, 370 (1984).
9. Stenger, H. G., *J. Catal.* 92, 426 (1985).
10. Iglesia, E., Reyes, S. C., Madon, R. J. and Soled, S. L., in "Advances in Catalysis" (D. D. Eley, H. Pines and P. B. Weisz, Eds.), Academic Press, Inc., Vol. 39, 1993, p. 221.
11. Puskas, I., Fleisch, T. H., Hall, J. B., Meyers, B. L., and Roginski, R. T., *J. Catal.* 134, 615 (1992).
12. Puskas, I., *Catal. Lett.* 22, 283 (1993).
13. Puskas, I., Meyers, B. L., and Hall, J. B., *Catalysis Today*, 21, 243 (1994).
14. Weisz, P. B., and Prater, C. D., in "Advances in Catalysis" (W. G. Frankenburg, V. I. Komarewsky and E. D. Rideal, Eds.), Academic Press, Inc., Vol. 6, 1954, p. 143.
15. Rajadhyaksha, R. A., and Doraiswamy, L. K., *Catal. Rev. - Sci. Eng.* 13, (20), 209, (1976).

FIGURE 1

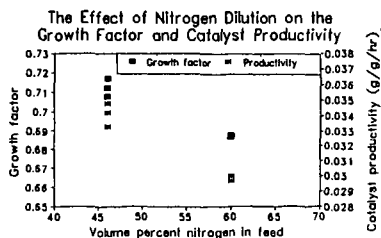


FIGURE 2

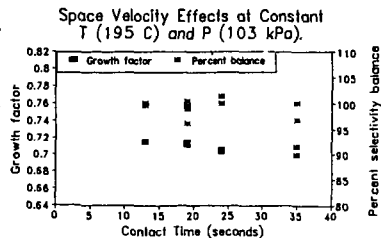


TABLE 1. Changes in Catalyst Performance and Product Selectivities with Changes in the H₂ to CO Feed Ratio.^a

H ₂ /CO ratio	2.0	2.0	2.5	2.5	3.1	3.1
VHSV	120	120	131	131	141	141
% CO conv.	60.3	59.4	77.3	77.5	91.5	93.5
Productivity	0.0285	0.0281	0.0367	0.0367	0.0436	0.0443
Growth factor	0.752	0.756	0.733	0.732	0.720	0.712
% Balance	96.2	95.8	93.1	93.9	96.6	97.7
% Selectivities						
CO ₂	2.9	2.8	2.6	2.7	2.2	2.7
C ₁	8.9	8.8	11.5	11.8	16.2	18.7
C ₂ -s	2.1	2.1	2.5	2.7	3.4	3.7
C ₃ -s	7.1	7.0	7.0	7.3	7.7	8.0
C ₄ -s	9.0	8.7	9.0	9.2	9.7	9.8
% of theoretical						
C ₁	151	153	167	171	213	233
C ₂ -s	24.4	24.6	26.4	28.0	34.1	32.4
C ₃ -s	69.7	70.0	66.1	68.5	71.4	73.4
Propene	38.8	39.8	23.2	23.1	9.0	6.5
Propane	30.8	30.2	42.9	45.4	62.4	66.9
C ₄ -s	87.2	85.8	87.1	89.1	93.3	95.7
1-Butene	23.7	23.5	14.7	14.8	9.8	9.9
n-Butane	33.6	33.1	42.6	43.8	58.9	62.8
t-2-Butene	14.3	13.7	16.2	16.6	14.9	14.5
c-2-Butene	15.6	15.5	13.7	13.9	9.7	8.5

^aCatalyst 1 at 197+1°C, 156 kPa. The volumetric feed compositions were 18-38-46, 16-41-43 and 15-47-38 CO-H₂-N₂, respectively.

TABLE 2. The Effect of Small Pressure Changes on Catalyst Performance and Product Selectivities.

Catalyst ID NO	2		4		5	
	203		193		202	
Temperature, °C						
Pressure, kPa	169	241	104	170	170	202
VHSV	131	131	286	286	220	220
Contact time (sec.)	46	65	13	21	27	32
% CO conversion	79.7	90.0	32.7	39.9	68.9	78.8
Productivity (g/g/hr)	0.034	0.039	0.014	0.016	0.043	0.050
Growth factor	0.703	0.736	0.739	0.789	0.648	0.696
% Balance	99.4	98.1	96.1	102.6	96.3	93.5
% CO ₂ selectivity	4.0	4.9	3.1	2.3	2.9	3.2
Selectivities, % of theoretical						
C ₁	144	142	191	215	135	122
C ₂	24.4	23.4	23.8	25.6	26.0	22.3
C ₃	68.1	65.6	69.6	76.5	70.4	62.8
Propene	22.8	21.4	40.0	44.7	25.8	21.2
Propane	45.2	44.2	29.5	31.7	44.5	41.6
C ₄	93.6	90.2	88.6	93.9	95.4	86.4
1-Butene	13.4	11.6	21.0	23.9	14.2	11.4
n-Butane	43.7	43.0	33.2	38.0	40.4	38.4
t-2-Butene	21.0	19.9	19.3	17.0	23.8	21.4
c-2-Butene	15.6	15.6	15.1	15.0	17.0	15.2

FIGURE 3

Space Velocity Correlation with CO Conversion and Catalyst Productivity

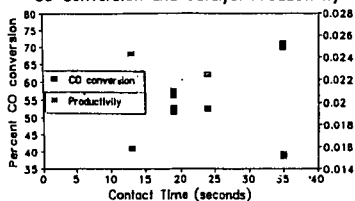


FIGURE 4

Contact Time-C₁ and C₂ Selectivity Correlations

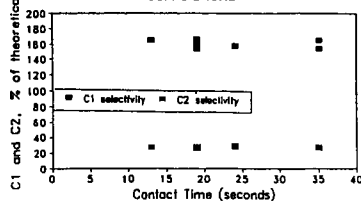


FIGURE 5
Contact Time-C3 Selectivity
Correlations

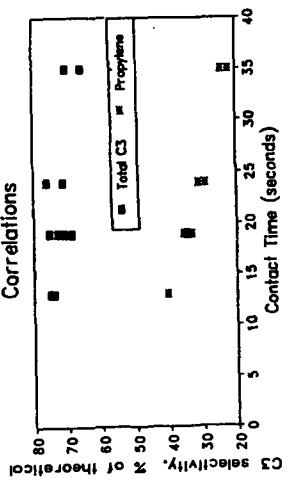


FIGURE 6
Contact Time-C4 Selectivity
Correlations

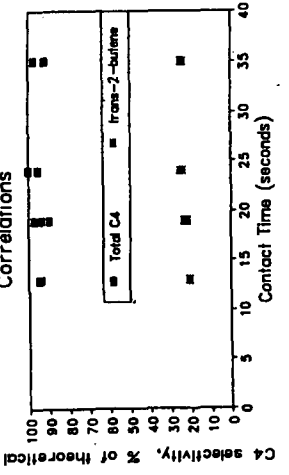


FIGURE 7

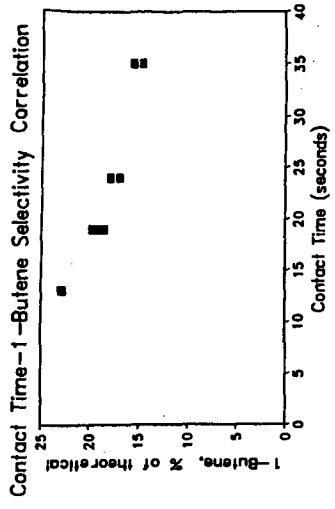


FIGURE 8
Contact Time-C4 Selectivity
Correlations

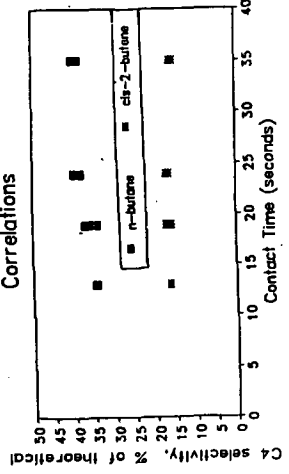


FIGURE 9
Growth Factors and Carbon Balances
versus T at Constant P and SV.

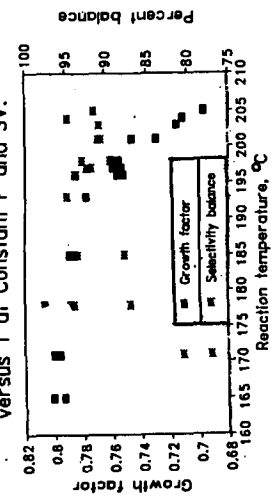


FIGURE 10

Correlation Between Temperature and the
C1 and C2 Selectivities.

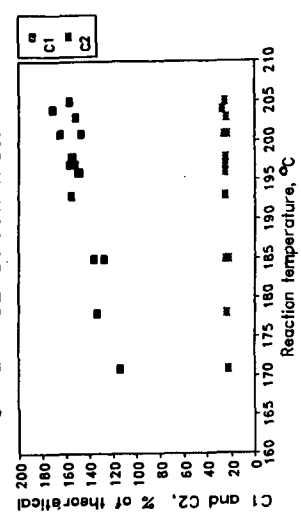


FIGURE 5
Contact Time-C3 Selectivity Correlations

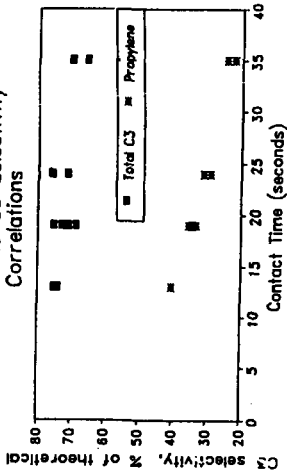


FIGURE 6
Contact Time-C4 Selectivity Correlations

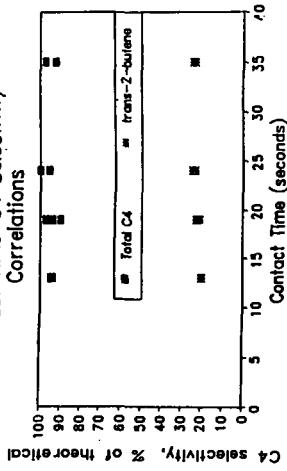


FIGURE 7

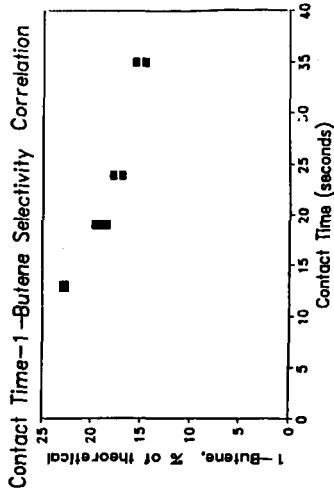


FIGURE 8
Contact Time-C4 Selectivity Correlations

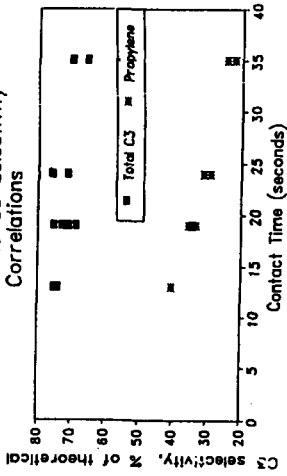


FIGURE 9
Growth Factors and Carbon Balances versus T at Constant P and SV.

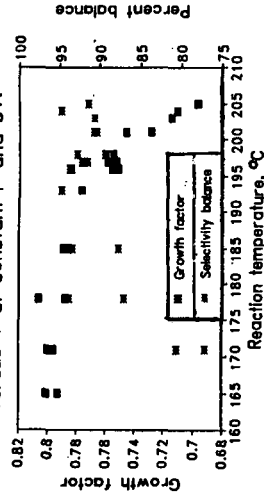


FIGURE 10
Correlation Between Temperature and the C1 and C2 Selectivities.

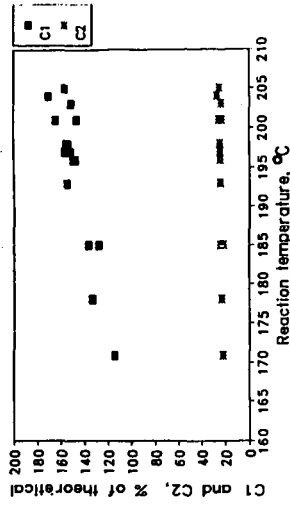


FIGURE 11

Correlation Between Temperature and the C3 Selectivities.

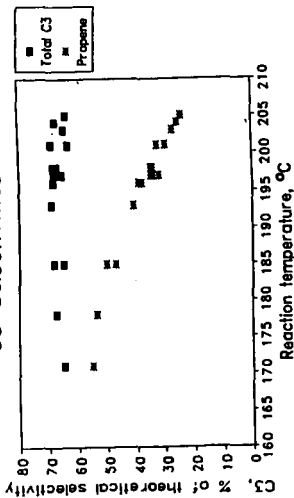


FIGURE 12

Correlation Between Temperature and the C4 Selectivities.

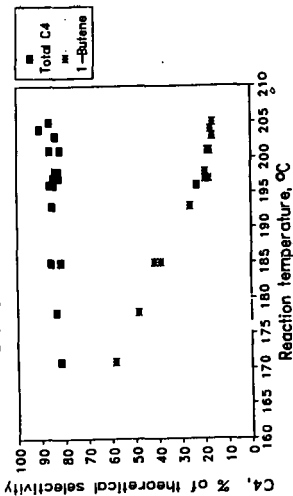


FIGURE 13

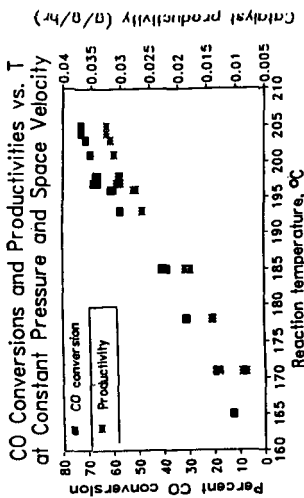


FIGURE 14. Arrhenius Plot.

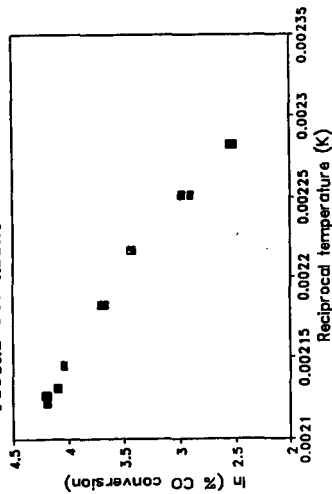


FIGURE 15. Calculated ASF Plot of a Product Distribution Continuously Changing in Alpha from 0.7 to 0.8

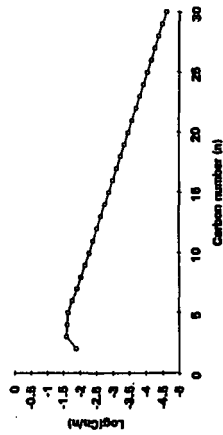


FIGURE 16. Calculated ASF Plots with Alpha Ranging from 0.60 to 0.85 and from 0.60 to 0.95

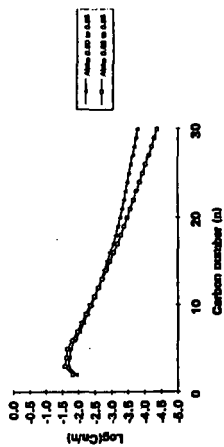


FIGURE 11

Correlation Between Temperature and the C3 Selectivities.

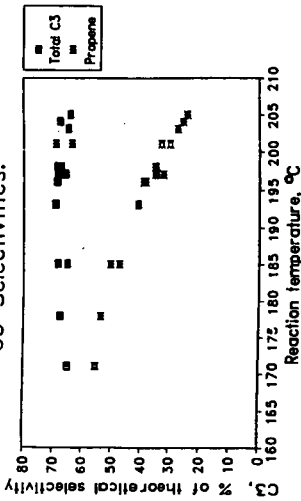


FIGURE 12

Correlation Between Temperature and the C4 Selectivities.

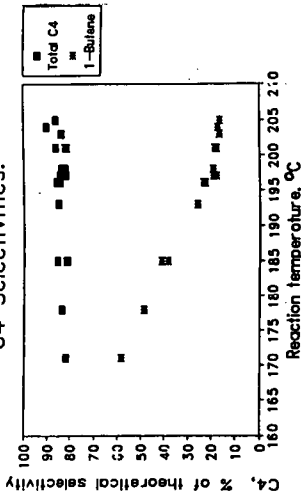


FIGURE 13

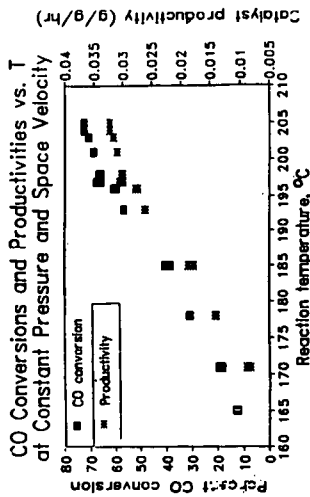


FIGURE 14. Arrhenius Plot.

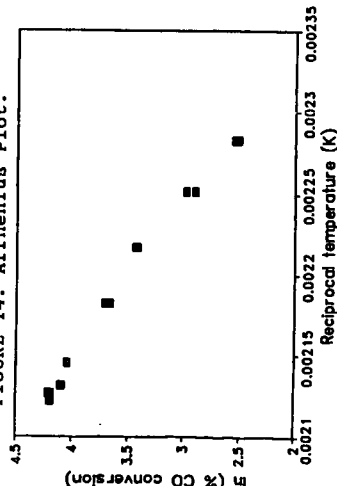


FIGURE 15. Calculated ASF Plot of a Product Distribution Continuously Changing in Alpha from 0.7 to 0.8

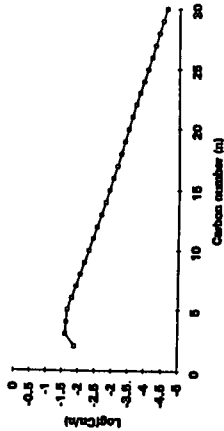


FIGURE 16. Calculated ASF Plots with Alphas Ranging from 0.60 to 0.85 and from 0.60 to 0.95

